TISSUE ENGINEERING: Part A
Volume 17, Numbers 15 and 16, 2011

DOI: 10.1089/ten.tea.2010.0550

Artificial Niche Combining Elastomeric Substrate and Platelets Guides Vascular Differentiation of Bone Marrow Mononuclear Cells

Wei Wu, Ph.D.,[1,2] Robert Allen, B.S.,[1] Jin Gao, Ph.D.,[1,2] and Yadong Wang, Ph.D.[1,2]

Bone marrow-derived progenitor cells are promising cell sources for vascular tissue engineering. However, conventional bone marrow mesenchymal stem cell expansion and induction strategies require plating on tissue culture plastic, a stiff substrate that may itself influence cell differentiation. Direct scaffold seeding avoids plating on plastic; to the best of our knowledge, there is no report of any scaffold that induces the differentiation of bone marrow mononuclear cells (BMNCs) to vascular cells *in vitro*. In this study, we hypothesize that an elastomeric scaffold with adsorbed plasma proteins and platelets will induce differentiation of BMNCs to vascular cells and promote vascular tissue formation by combining soft tissue mechanical properties with platelet-mediated tissue repairing signals. To test our hypothesis, we directly seeded rat primary BMNCs in four types of scaffolds: poly(lactide-co-glycolide), elastomeric poly(glycerol sebacate) (PGS), platelet-poor plasma-coated PGS, and PGS coated by plasma supplemented with platelets. After 21 days of culture, osteochondral differentiation of cells in poly(lactide-co-glycolide) was detected, but most of the adhered cells on the surface of all PGS scaffolds expressed calponin-I and α-smooth muscle actin, suggesting smooth muscle differentiation. Cells in PGS scaffolds also produced significant amount of collagen and elastin. Further, plasma coating improves seeding efficiency, and platelet increases proliferation, the number of differentiated cells, and extracellular matrix content. Thus, the artificial niche composed of platelets, plasma, and PGS is promising for artery tissue engineering using BMNCs.

Introduction

Ischemic heart disease is the leading cause of death worldwide. Coronary bypass surgery can reperfuse the ischemic heart and significantly reduce mortality.[1] Autografts are the standard of care for bypass grafting, but many patients lack suitable autografts.[2] Tissue engineered blood vessels produced from autologous cells could be used for bypass *in lieu* of autografts.[3–5] However, challenges in blood vessel engineering include maintaining antithrombogenicity, matching arterial compliance, and identifying clinically feasible cell sources.

Bone marrow cells are a promising source for blood vessel tissue engineering because they include multiple progenitor populations capable of vascular differentiation.[6–8] Clinical application of bone marrow mononuclear cell (BMNC)-seeded grafts as venous conduits in congenital heart surgery demonstrated excellent safety profiles and 100% patency rates at 1–3 years of follow-up.[5,9] Animal experiments showed that bone marrow stromal cells (BMSCs) could act as supporting cells for endothelial progenitor cells (EPCs) and form long-lasting functional microvasculature.[10] Typical use of bone marrow-derived cells in vascular tissue engineering calls for plating the cell mixture on tissue culture plastic to first isolate the adhered subpopulation, also known as BMSCs, first. BMSCs are then induced to differentiate to vascular cells before scaffold seeding.[11,12] However, repeated enzymatic digestion, long periods of cell expansion, expense of various growth factors, and possible interferences of cell behavior caused by supra-physiologic stiffness of Petri dishes remain problems to be resolved.[13] Direct seeding of BMNCs instead of BMSCs into the desired scaffolds bypasses the Petri dish adhesion step and therefore may be advantageous for cell viability, maintenance of cell phenotype, and simplifying *in vitro* procedures.

Poly(glycerol sebacate) (PGS) is a degradable, biocompatible, and elastomeric polyester with a Young's modulus comparable to that of native arteries ($E = 0.282$ MPa[14]) The modulus is within the range of elastic moduli found for small diameter arteries in large mammals.[15,16] Our previous work demonstrated that vascular smooth muscle cells (SMCs) grown on PGS scaffolds showed elastin expression and

[1]Department of Bioengineering, University of Pittsburgh, Pittsburgh, Pennsylvania.
[2]McGowan Institute of Regenerative Medicine, University of Pittsburgh, Pittsburgh, Pennsylvania.

compliance more similar to native vessels than those grown on stiffer but chemically similar poly(lactic-co-glycolic acid) (PLGA) scaffolds.[17] Further, Sales *et al.* demonstrated that precoating natural matrix onto PGS scaffolds would enhance EPC expression of functional proteins and extracellular matrix (ECM).[18] The above results suggest that establishing a microenvironment with mechanical and biochemical characteristics similar to those of blood vessels can improve vascular tissue formation from either mature or progenitor cells.

Platelets have been identified to contain multiple growth factors and are involved in tissue healing and repair. Accumulating evidence suggests that platelets play an essential role in recruiting circulating EPCs by paracrine release of stem cell-derived factor-α and vascular endothelial growth factor.[19,20] Additionally, platelet-rich plasma has been shown clinically to promote wound healing and enhance bone and tendon repair.[21] Consequently, we hypothesized that incorporating both plasma proteins and platelets in an elastomeric PGS scaffold could provide a microenvironment inducive of BMNC proliferation and differentiation to vascular cells and support subsequent vascular tissue formation. In this study, we produced this "artificial niche" for vascular tissue formation (Fig. 1) and investigated the effects of substrate elasticity, plasma precoating, and platelet preadhesion on the adhesion, proliferation, and differentiation of directly seeded BMNCs. We show that BMNCs can adhere, proliferate, and differentiate into smooth-muscle like cells, and that these cells synthesize collagen III and elastin, hallmark ECM proteins of blood vessels.

Materials and Methods

Animal care procedures were conducted in appliance with National Institutes of Health (NIH) guidelines (NIH publication no. 85–23 rev. 1985) and approved by the Institutional Animal Care and Use Committees at the University of Pittsburgh. Male Sprague Dawley rats (200–250 g) were used for bone marrow and platelet harvesting.

Isolation of platelet-poor plasma and platelets

Platelet-poor plasma and platelets were isolated according to previously published literature with minor modifications.[16] Briefly, to isolate platelet-poor plasma, whole blood was aspirated from rat hearts and anticoagulated by low-molecular-weight heparin (20 U/mL, low-molecular-weight heparin; MP Biotech, Solon, OH). Blood was then centrifuged at 1200 *g* for 10 min at 22°C to separate blood cells and platelets from plasma. Plasma was diluted with phosphate-buffered saline (PBS) to 20% of the original concentration to slow fibrin polymerization when used as a scaffold coating, thereby improving fibrin infiltration within scaffold pores. To isolate platelets, whole blood from rat hearts was drawn into a syringe containing 3.8% sodium citrate (volume ratio, blood:sodium citrate = 9:1) to prevent coagulation. To remove erythrocytes, blood was centrifuged at 420 *g* for 10 min at 22°C, and plasma containing platelets was transferred to another centrifuge tube. Plasma containing platelets was centrifuged at 1200 *g* for an additional 10 min at 22°C to concentrate platelets. To produce platelet-supplemented plasma, platelet pellets were resuspended in diluted platelet-poor plasma at a density of 1.0×10^9/mL.

Isolation of BMNCs

BMNCs from two rats were pooled and seeded into three scaffolds in each group. BMNCs were isolated from rat femurs and tibias immediately after euthanization. Briefly, both ends of the bones were severed, and marrows were flushed from bones with heparinized (100 U/mL) PBS. Fat and bone fragments were removed by a 100 μm filter. To isolate BMNCs, filtered marrow was centrifuged on a histopaque density gradient (Sigma-Aldrich, St. Louis, MO) at 2700 rpm for 20 min.

Preparation of the tissue engineered constructs

For scaffold fabrication, PGS was dissolved in tetrahydrofuran (20%), and salt fusion and particulate leaching methods were used to fabricate porous scaffold (thickness = 1.0 mm, pore size = 75–100 μm, porosity ≥90%) as previously,[22,23] and the compressive modulus of the scaffolds was 4.05 ± 1.30 KPa as previously reported.[22] Scaffolds were cut into 1 cm^2 sheets (strips or disks) and autoclaved. Scaffolds were purified by serially soaking in 75%, 50%, and 30% ethanol, followed by soaking in PBS. To coat PGS with platelet-poor plasma (P-PGS), 150 μL of platelet-poor plasma was applied to the surface of PGS scaffolds. Scaffolds were then incubated at 37°C for 15 min, and subsequently rinsed with PBS to remove excess plasma. To coat PGS scaffolds with platelet-supplemented plasma (Pl-P-PGS), platelet supplemented plasma was applied using the same protocol as described for platelet-poor plasma coating.

Scaffolds were seeded with BMNCs by dynamic rotational cell seeding as previously described.[24] Briefly, cells (1.5×10^6

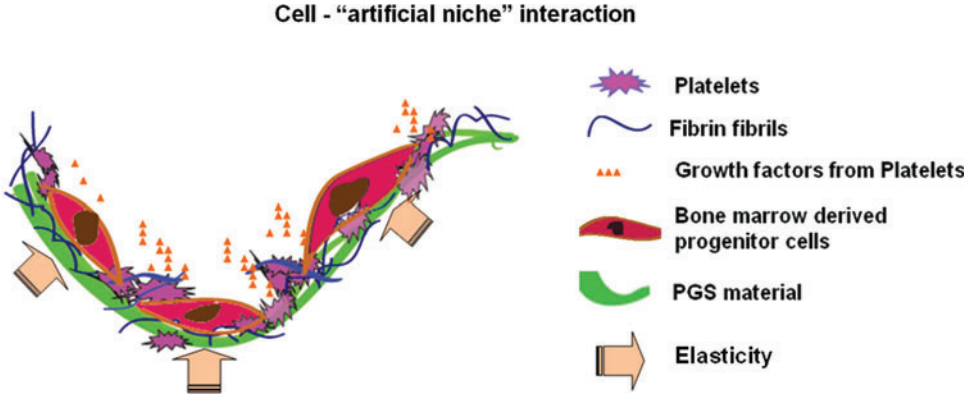

FIG. 1. Components of the artificial niche: elastomeric PGS scaffolds coated with fibrin and platelets constitute the artificial niche. Bone marrow mononuclear cell adhesion, vascular differentiation, and proliferation are mediated by the elasticity of PGS and biochemical signals from fibrin and platelet. PGS, poly(glycerol sebacate). Color images available online at www.liebertonline.com/tea

cells/cm^2 scaffold) suspended in 10 mL culture medium were seeded on scaffolds of each group in disposable scintillation vials (Wheaton, Millville, NJ; 20 mL) and rotated at 2 rpm at 37°C for 48 h in a hybridization chamber. The slow rotational speed allows longer contact between cells and scaffolds than at higher speeds, and prevents settling of the cells by gravity. Culture medium consisted of MCDB 131 (Mediatech, Hernton, VA) supplemented with 10% (v/v) fetal bovine serum (FBS; Lonza, Basel, Switzerland), 50 mg/L ascorbic acid (Sigma-Aldrich), and 20 μM L-glutamine (Mediatech). Culture medium was replaced at 4 and 12 h. After seeding, constructs were cultured for 19 days in a modified spinner-flask bioreactor to minimize gradients in the culture medium (Fig. 2). The bioreactor consists of a 50 mL glass beaker containing a magnetic stir bar under a stainless steel mesh platform. Constructs were fixed on the stainless steel mesh platform near the wall of the beaker. Three constructs in the same experimental group were spaced equidistant from one another in each bioreactor. The magnetic stirrer stirs at 20 rpm continuously to facilitate diffusion of culture medium. Culture medium was changed every 3 days. As control group, PLGA scaffolds made from the same salt leaching method were cut into the same size as PGS above, then seeded with BMNCs and cultured under the same conditions. Another control group was also set up by seeding bamboo SMCs in PGS scaffolds (Supplementary Fig. S1; Supplementary Data are available online at www.liebertonline.com/tea).

Examination of cell adhesion and proliferation

After 15 h of rotational cell seeding, scaffolds were fixed with 10% formalin and stained with 4′,6-diamidino-2-phenylindole (DAPI; Sigma, St. Louis, MO) to observe cell nuclei. Stained cells were observed and counted using a fluorescent microscope. To observe cell infiltration during cell seeding process, the samples were frozen into Tissue-Tek optimal cutting temperature compound (O.C.T.; Sakara Finetek, Torrance, CA), cryosectioned to 8 μm thickness, and stained with hematoxylin and eosin (H&E).

For quantification of cells captured by scaffolds, crystal violet staining was performed as previously described.[17] Briefly, each freshly seeded construct ($n=5$) was rinsed with PBS, then finely minced with surgical scissors. Scaffold pieces were transferred to a 15 mL centrifuge tube and rinsed twice with filtered crystal violet solution. Each tube was vortexed to free as many cell nuclei as possible from the scaffold and then incubated at 37°C for 48 h. To confirm adequate liberation of cell nuclei, the largest scaffold fragments were compressed repeatedly using forceps, and microscopic observation showed no release of additional nuclei. The number of cell nuclei was counted under a Nikon TiE microscope.

DNA content was used to quantify cell proliferation rather than crystal violet staining because ECM deposition prevented the complete removal of cell nuclei. Total DNA was quantified for constructs ($n=5$) incubated for 3 days and 10 days using TRIzol® reagent according to the manufacturer's protocol (Invitrogen, Carlsbad, CA; Briefly, constructs were minced with surgical scissors and extracted in the TRIzol reagent). After DNA isolation and washing procedures, total DNA was measured by absorbance at 260 nm by a BioTek Synergy-MX spectrophotometer.

To quantify the amount of biological tissue made by the cells, wet constructs ($n=3$ in each group) were weighed and then subjected to TRIzol digestion for 20 min at room temperature. The constructs were rinsed with PBS and centrifuged at 200 rpm for 1 min to remove residual tissues. The wet weights of the constructs were again recorded and compared to the wet weights before digestion.

Scanning electron microscopy

Samples were fixed in 2.5% (v/v) glutaraldehyde and dehydrated in a graded series of ethanol solutions (25%, 30%, 50%, 60%, 70%, 80%, and 90% ethanol) for 20 min each, followed by three subsequent dehydrations in 100% ethanol and hexamethyldisilazane. Samples were then mounted on aluminum stubs, gold sputtered, and imaged using a JEOL JSM6330F scanning electron microscope (SEM) (Tokyo, Japan).

Histology and immunohistochemistry

Histological analysis and characterization of cell phenotypes were performed as previously described.[20] To determine overall construct morphology for PGS constructs, constructs were embedded in O.C.T, cryosectioned to 8 μm thickness, and stained with H&E or Masson's trichrome (MTS). To estimate cell density of PGS constructs from H&E micrographs, total nuclei per cm^2 of longitudinal construct sections were counted from representative images at 100× magnification using Nikon Elements Software ($n=6$).

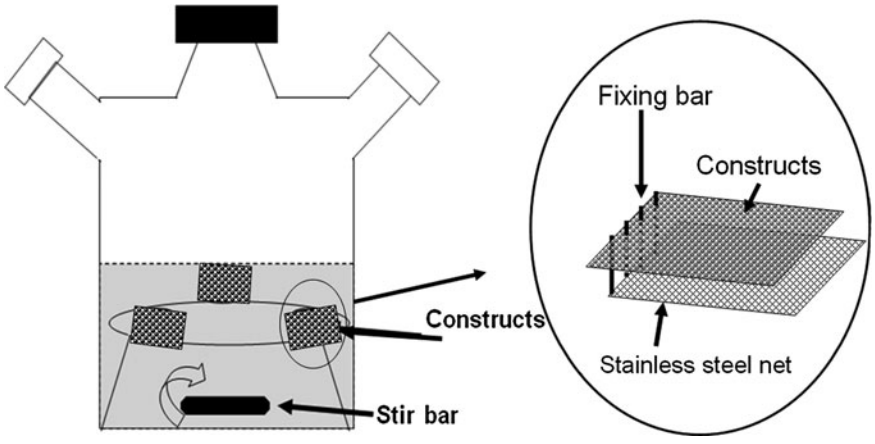

FIG. 2. Scheme of the spinning culture systems. Constructs were secured in stainless steel meshes and fixed near the edge of culture vessels. A magnetic stir bar was used to circulate culture medium (MCDB131 containing 10% fetal bovine serum, 50 mg/L ascorbic acid, and 20 μM L-glutamine).

Table 1. Antibodies Used for Immunofluorescent Staining

Antibody	*Species*	*Working concentration*	*Company*
Anti α-SMA	Mouse × Rat	1:40	Sigma-Aldrich, St. Louis, MO
Anti Calponin-I	Mouse × Rat	1:200	Abcam, San Francisco, CA
Anti–vWF	Rabbit × Rat	1:400	Abcam, San Francisco, CA
Anti Elastin	Rabbit × Rat	1:40	Millipore, Billerica, MA
Anti Collagen III	Rabbit × Rat	1:100	Abcam, San Francisco, CA
Alexa 594 IgG	Goat × Rabbit	1:800	Invitrogen, Carlsbad, CA
Alexa 488 IgG	Rabbit × Mouse	1:800	Invitrogen, Carlsbad, CA

α-SMA, α-smooth muscle actin; VWF, von Willebrand factor.

To characterize osteogenesis in the constructs, all of the samples were processed for von Kossa staining. In addition, alkaline phosphate (ALP) activity was quantified in constructs cultured for 14 days as follows: Samples were minced and lysed using Cellytic™ cell lysis reagent (Sigma; 300 μL/sample); then the solution was centrifuged at 12,000 rpm (10,800 *g*) at 4°C for 15 min, and the supernatant solution was collected. Protein content was quantified by adding protein assay reagent (Pierce 660 nm). ALP yellow liquid substrate system for ELISA was used to quantify ALP content in the samples, total ALP content was measured by absorbance at 405 nm using a BioTek Synergy-MX multiplate reader.

Immunofluorescence microscopy was used to observe platelets, determine cell phenotypes, and identify ECM proteins in PGS constructs. Antibodies for immunofluorescence microscopy are summarized in Table 1. To identify platelets, Pl-P-PGS scaffolds and constructs were immunostained using von Willebrand factor primary antibodies. To assess cell phenotypes, constructs were immunostained for SMC markers α-smooth muscle actin (α-SMA) and calponin-I, which are early and middle stage differentiation markers, respectively. To identify elastin and collagen III, ECM proteins characteristic of vascular tissues, immunostaining was performed. Immunostaining was performed as follows: Frozen sections were fixed in acetone for 10 min and then air dried. Nonspecific binding was blocked by 30 min incubation in normal goat serum (5% v/v, 0.1% Triton × 100, 0.1 M PBS, pH 7.4). Slides were then incubated in the primary antibodies for 40 min at 37°C. Slides were subsequently rinsed three times in PBS, and then blocked again in normal goat serum. Slides were then incubated with fluorescein isothiocyanate-conjugated secondary antibodies for 30 min at room temperature and rinsed three times with PBS. Slides were co-stained for nuclei with DAPI (Invitrogen). Negative controls were stained using the same protocol but without primary antibodies. Positive controls were

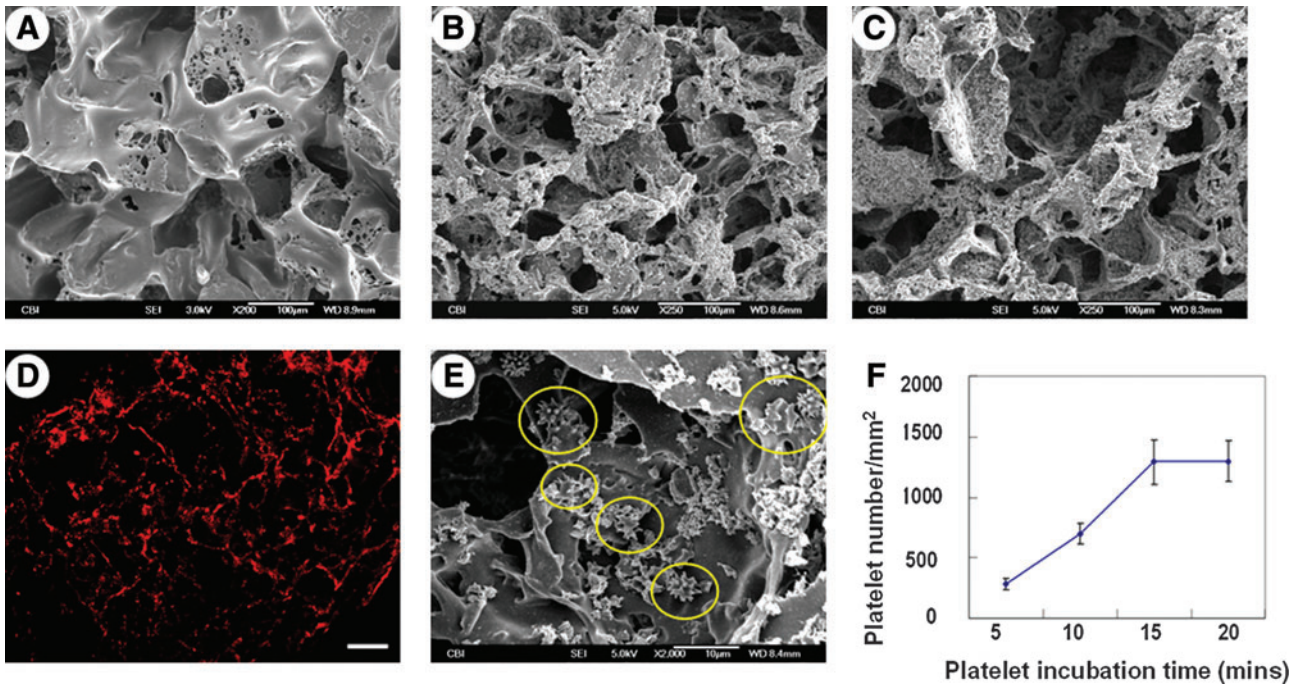

FIG. 3. Characterization of scaffolds. **(A)** SEM micrographs of PGS scaffolds showed high porosity and good interconnectivity between pores. Scale bar = 100 μm. **(B)** Platelet-poor plasma and **(C)** platelet-poor plasma-coated scaffolds displayed plasma deposition in the interior surfaces. Scale bars = 100 μm. **(D)** Anti–von Willebrand factor immunofluorescent staining of Pl-P-PGS cross sections demonstrate wide distribution of platelets throughout the Pl-P-PGS scaffold. 100×, scale bar = 100 μm. **(E)** Adherent platelets on Pl-P-PGS scaffolds extended multiple processes characteristic of activated platelets. Scale bar = 10 μm. **(F)** Platelet adhesion increased with time and plateaued at 15 min incubation. Pl-P-PGS, PGS scaffolds with platelet supplemented plasma. SEM, scanning electron microscope. Color images available online at www.liebertonline.com/tea

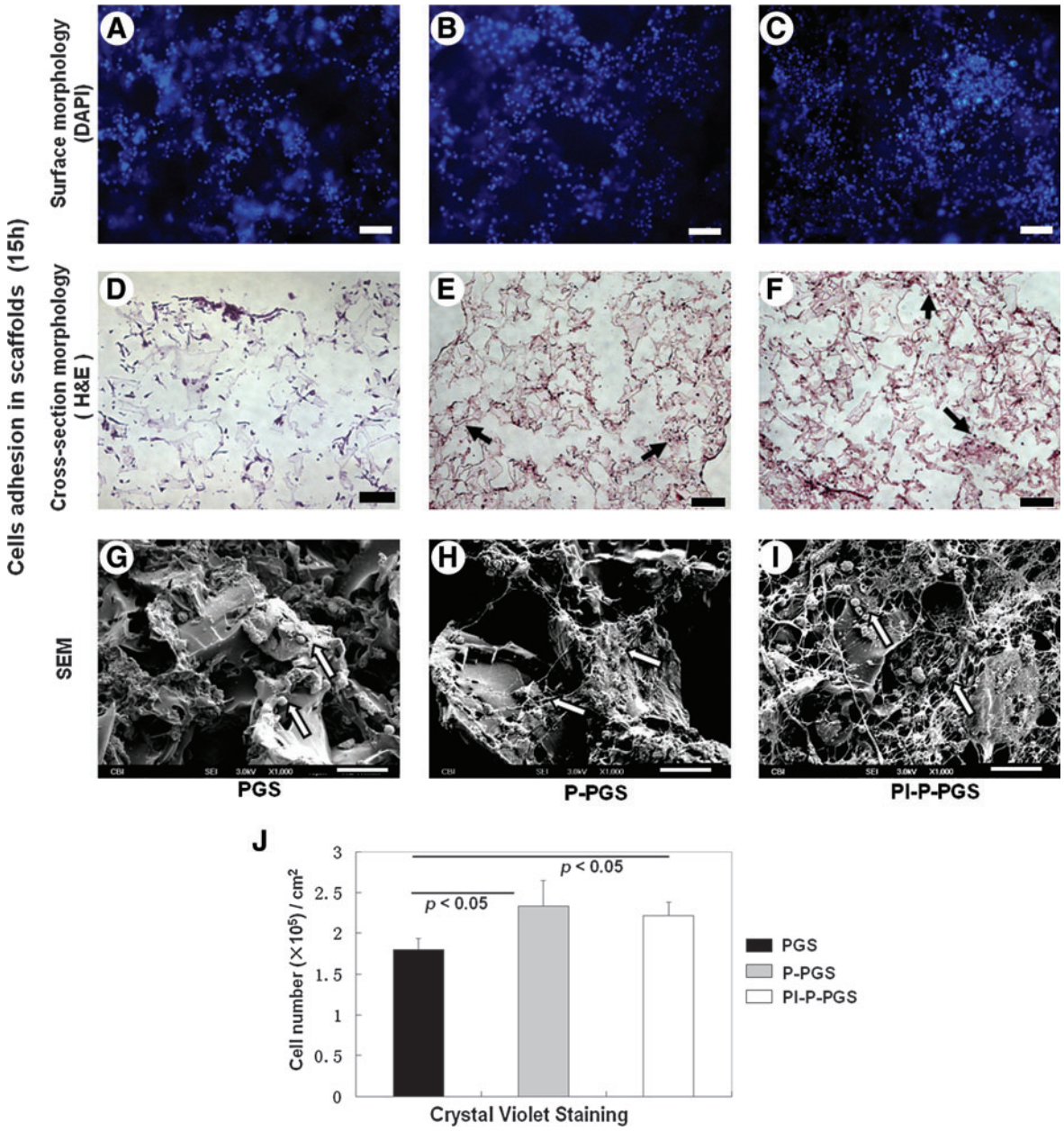

FIG. 4. Cell capture by PGS scaffolds. **(A)** and **(D)** are representative images of PGS scaffolds, **(B)** and **(E)** of P-PGS, and **(C)** and **(F)** of Pl-P-PGS. After 15 h of rotational cell seeding, constructs were stained with DAPI to observe cells on the scaffold surface **(A–C)**, and cross sections of constructs were stained with H&E to observe cells in the interior of the scaffolds **(D–F)**. Arrows indicate stained cell nucleus (dark purple points) distributed in scaffolds. Scale bars equal 100 μm for images **(A–F)**. **(G–I)** SEM images showed detailed morphology of cells on the surface of the scaffolds; arrows indicate attached cells. 100×, scale bars equal 20 μm. **(J)** The number of cells adhered in scaffolds was quantified using crystal violet staining, $n=5$, $p<0.05$. P-PGS and Pl-P-PGS scaffolds had significantly higher cell seeding efficiency than bare PGS. H&E, hematoxylin and eosin. Color images available online at www.liebertonline.com/tea

stained from constructs seeded with adult baboon arterial SMCs (passages 4 to 5) cultured under the same conditions. All the stained sections were analyzed using an inverted Nikon TiE microscope and Nikon NIS-Elements software (Nikon Instruments, Melville, NY).

Western blotting

Engineered tissues were crushed manually and dissolved in a lysis buffer (pH 7.4) containing 25 mM Tris base, 0.4 mM sodium chloride, 0.5% (w/v) sodium dodecyl sulfate, and a protease inhibitor cocktail (Sigma) to extract proteins. Protein concentrations were quantified by Bradford assay using Quick Start Bradford Dye Reagents (Bio-Rad, Hercules, CA). Cell lysates (30 μg) were size fractioned by sodium dodecyl sulfate–polyacrylamide gel electrophoresis, and western blotting was performed with selective β-actins (1:500; Sigma), calponin-I (1:500; Abcam), and α-SMA (1:1000; Millipore, Billerica, MA). The bands were further quantified using NIH ImageJ.

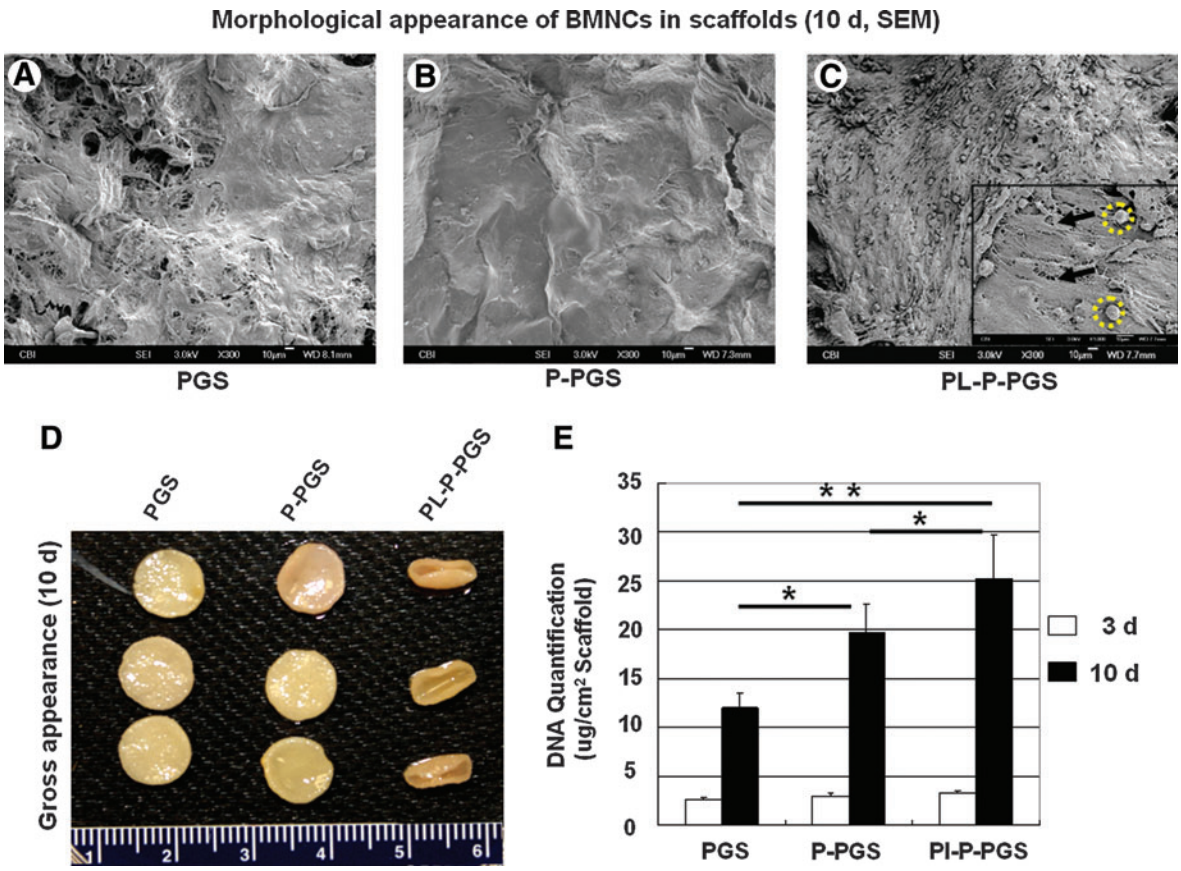

FIG. 5. Characterization of cell proliferation in scaffolds after 10 days of culture. SEM micrographs revealed adherent cells on the surface of the scaffolds: **(A)** PGS, **(B)** P-PGS, and **(C)** Pl-P-PGS scaffolds. Pl-P-PGS constructs exhibited more cells on the surface than the other groups. Inset: higher magnification (1000×). Two distinct cell morphologies are present: spread, spindle-like cells (arrows) and more spherical cells (dotted circles). **(D)** Macroscopic examination showed that Pl-P-PGS constructs deformed the most. **(E)** DNA quantification shows significantly increased proliferation in Pl-P-PGS scaffolds compared with P-PGS and uncoated PGS, $n=5$, $^{*}p<0.05$, $^{**}p<0.01$. Color images available online at www.liebertonline.com/tea

Quantitative biochemical matrix analysis

Insoluble elastin content was determined for constructs ($n=4$ in each group) using a Fastin™ Elastin Assay Kit (F2000; Biocolor, Carrickfergus, United Kingdom). Insoluble elastin was extracted from constructs by mincing construct segments (length 5 mm) into pieces no larger than 1.0 mm^2 and digesting with oxalic acid at 60°C. Elastin concentration in the supernatant was measured using the kit instructions, and total elastin per construct wet weight was calculated from the elastin standard curve.

Collagen content was quantified using a Sircol™ Collagen Assay (S1000; Biocolor). Collagen was extracted from constructs ($n=4$ in each group) by mincing construct segments and digesting pieces with 0.5 M acetic acid containing 1 mg/mL pepsin A. Collagen concentration in the supernatant was measured following kit instructions, and total collagen per construct wet weight was calculated from the collagen standard curve. For normalization of biochemical contents in constructs, the DNA contents were also quantified from part of same samples or constructs in the same bioreactor. The collagen and elastin contents were normalized to per microgram DNA.

Statistical analysis

All results are expressed as mean ± standard deviation. Statistical analyses were performed using SPSS 17.0 software (SPSS, Inc., Chicago, IL). ANOVA was used for multiple group comparisons followed by Tukey's Honestly Significant Difference or Games-Howell post tests. A p-value <0.05 was considered significant (Supplementary Tables S1 and S2).

Results

Scaffold morphology

SEM examination of PGS scaffolds revealed high porosity and pore interconnectivity (Fig. 3A). SEM for P-PGS and Pl-P-PGS groups immediately after coating are shown in Figure 3B and C, respectively. Pl-P coating deposited platelets (Fig. 3D, E) evenly in the scaffolds. Adherent platelets extended multiple processes, characteristic of activated platelets (Fig. 3E). Platelet adherence reached a plateau after 15 min of incubation (Fig. 3F).

Platelet-poor plasma enhances cell seeding efficiency in scaffolds

Constructs were examined with DAPI staining, H&E staining, crystal violet staining, and SEM to assess cell capture after 15 h of rotational cell seeding. DAPI and H&E micrographs showed cell adhesion in all PGS scaffolds (Fig. 4A–F). Further, H&E staining of the cross section of the constructs indicated good cell penetration into the bulk of the

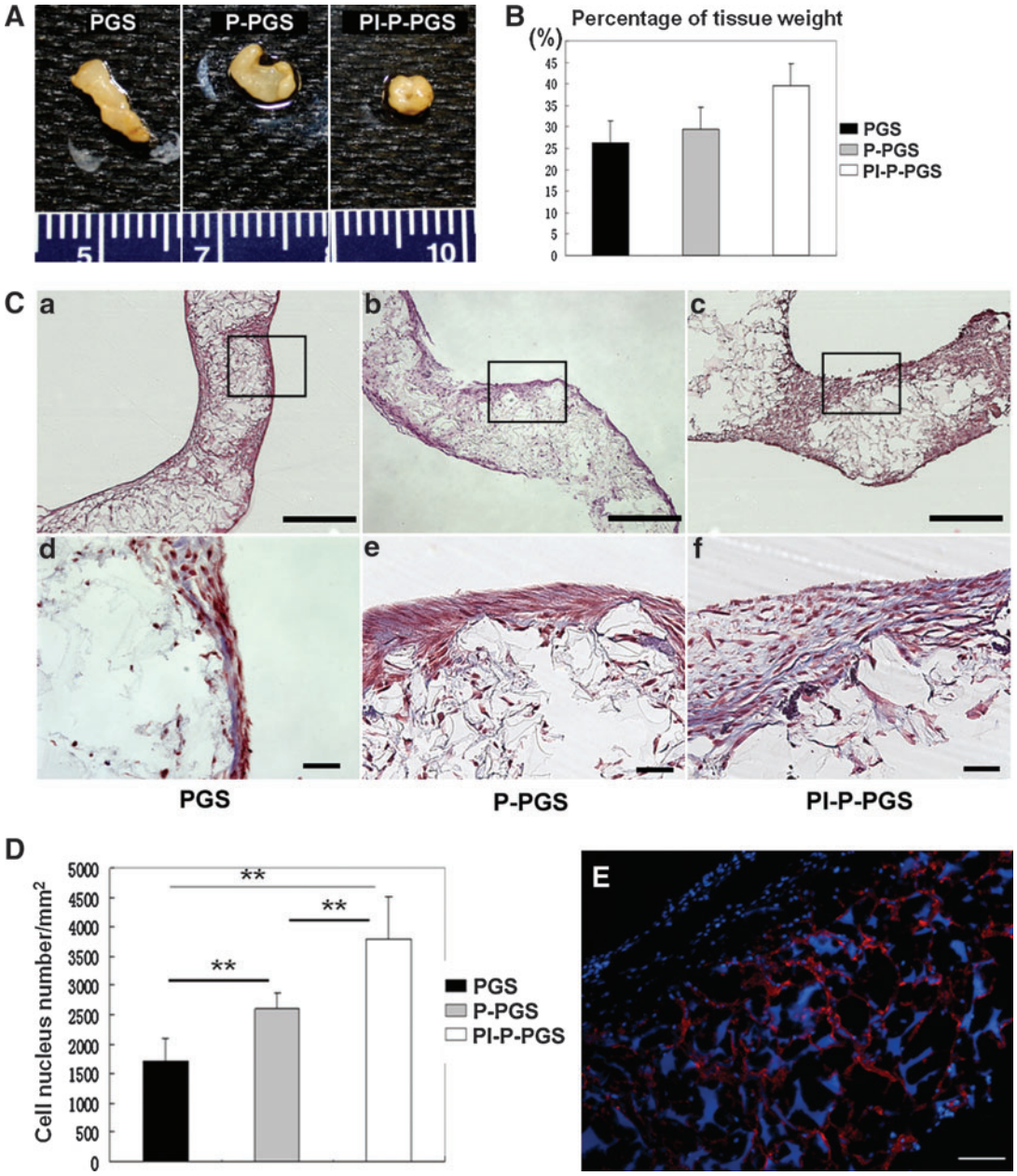

FIG. 6. Construct tissue formation after 21 days of culture. **(A)** Macroscopic images showed more drastic construct deformation for all constructs than day 10. Ruler ticks = 1 mm. **(B)** Wet weight percentage of biologic tissues in constructs ($n = 3$). **(C)** Histological evaluation of the constructs (**a–c**: H&E staining, 40×, scale bars = 500 μm. **d–f**: MTS, 200×, scale bars = 50 μm). **(D)** Cell density of the constructs approximated by nucleus counting of construct cross sections using Nikon Elements software ($n = 6$). Pl-P-PGS group demonstrated significantly higher cell density than the other groups. Values represent mean ± standard error, $^{**}p < 0.01$. Analysis performed in triplicate. **(E)** Immunofluorescent images of anti–von Willebrand factor staining revealed that platelets (red) were still present in Pl-P-PGS constructs after 21 days. DAPI co-staining (blue) labeled cell nuclei and is also nonspecifically adsorbed by PGS. 100×, scale bars = 100 μm. MTS, Masson's trichrome; DAPI, 4′,6-diamidino-2-phenylindole. Color images available online at www.liebertonline.com/tea

constructs (Fig. 4D–F). SEM indicated good cell adhesion on the construct surfaces (Fig. 4G–I). In P-PGS and Pl-P-PGS constructs, cells appeared to be closely associated with fibrin cables. Indeed, nuclei counting indicated that P-PGS and Pl-P-PGS scaffolds had significantly higher seeding efficiency than uncoated PGS scaffolds (Fig. 4J). There was no significant difference in seeding efficiency between Pl-P-PGS and P-PGS.

Platelet-poor plasma and platelets improve BMNC proliferation

Gross appearance, SEM examination, and DNA quantification indicated that platelet-poor plasma and platelet coating improved BMNC proliferation. SEM of constructs cultured for 10 days demonstrated that PGS and P-PGS scaffolds supported a sub-confluent and confluent cell

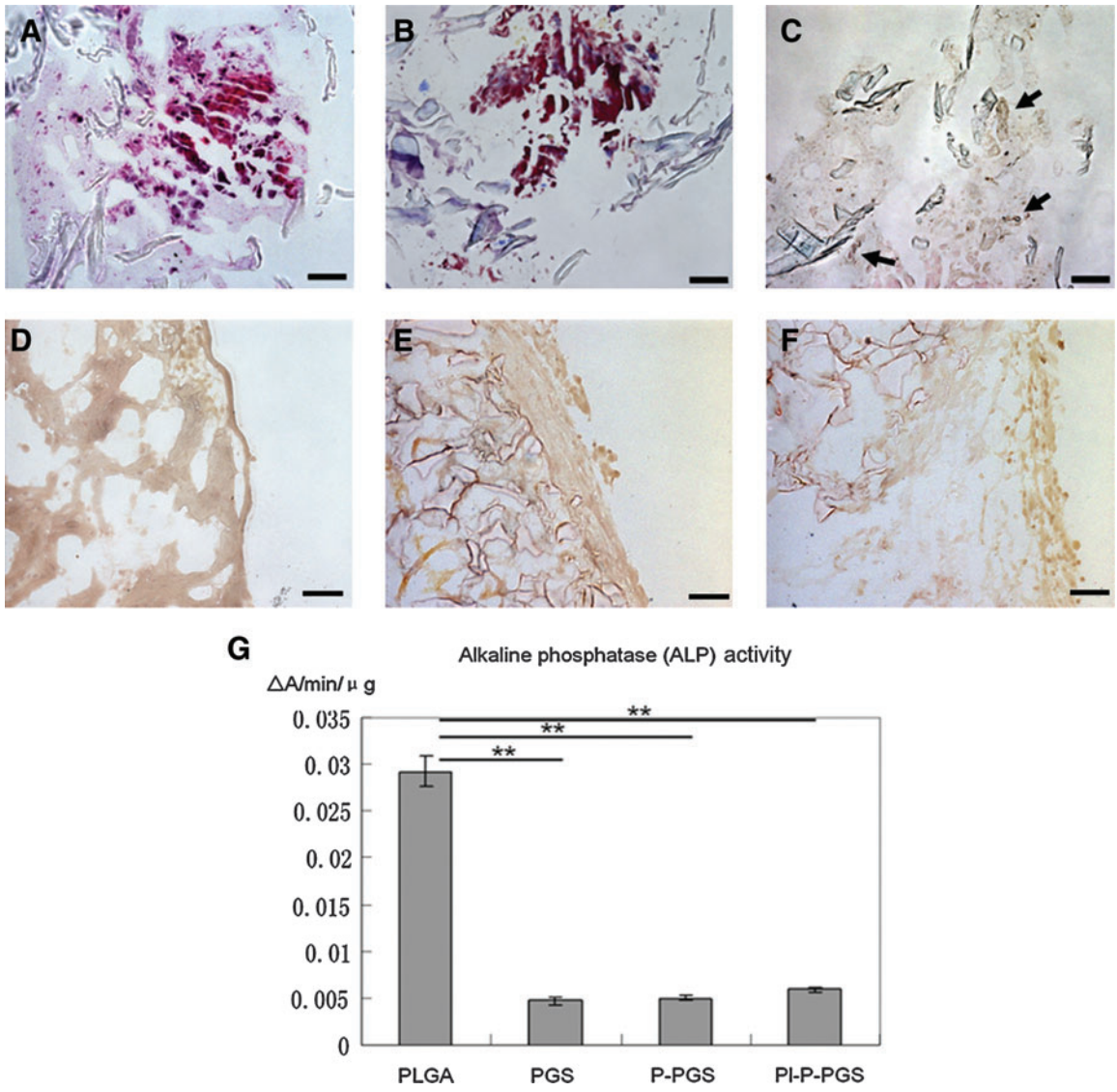

FIG. 7. **(A–C)** H&E, Masson's trichrome, and von Kossa staining of PLGA constructs indicated calcification distributed sparsely in the constructs (dark spots, indicated by arrows). 200×, scale bars = 100 μm. **(D–F)** In contrast, staining for PGS, P-PGS, and Pl-P-PGS showed no calcium deposition. 200×, scale bars = 100 μm. **(G)** Quantification of ALP activity in all groups indicated that cells in PLGA scaffold have significantly higher ALP activity than those in all PGS groups, $n = 4$, $^{**}p < 0.01$. PLGA, poly(lactic-co-glycolic acid); ALP, alkaline phosphate. Color images available online at www.liebertonline.com/tea

monolayer, respectively (Fig. 5A, B), whereas Pl-P-PGS scaffolds supported multiple layers of cells on the scaffold surface (Fig. 5C). Interestingly, two distinct cellular morphologies were observed—spread, spindle-like cells and more spherical cells (Fig. 5C). Enhanced cellularity caused by platelet coating was also reflected macroscopically, Pl-P-PGS constructs contracted the most (Fig. 5D), likely because larger numbers of exerted larger traction forces on the scaffolds. To further investigate cell proliferation, DNA quantification of the constructs was used (Fig. 5E). Platelet-poor plasma and Pl-P coatings both significantly increased cellularity compared to uncoated PGS at day 10 ($p < 0.01$). Additionally, Pl-P coating significantly improved cellularity further than platelet-poor plasma alone ($p < 0.05$), suggesting that adding platelets to plasma coating enhanced cell proliferation.

Platelets promote tissue formation

Constructs remodeled significantly during 21 days of culture. Although all constructs showed more deformation than day 10, Pl-P-PGS constructs deformed most drastically (Fig. 6A). Further, the tissue wet weight measurement indicated that the mean values of the weight ratio of biologic tissues and construct were the highest for Pl-P-PGS, second highest for P-PGS, and the lowest for PGS (Fig. 6B). However, no statistically significant differences in percent tissue weight was detected, $p = 0.098$. H&E staining of the specimens showed differences in cell distribution and scaffold structure between the 3 groups (Fig. 6C, top panel). In PGS and P-PGS scaffolds, multilayers of cells covered the scaffold surface, with cells present within scaffold pores. Thicker cell aggregates appeared to form on the surface of Pl-P-PGS

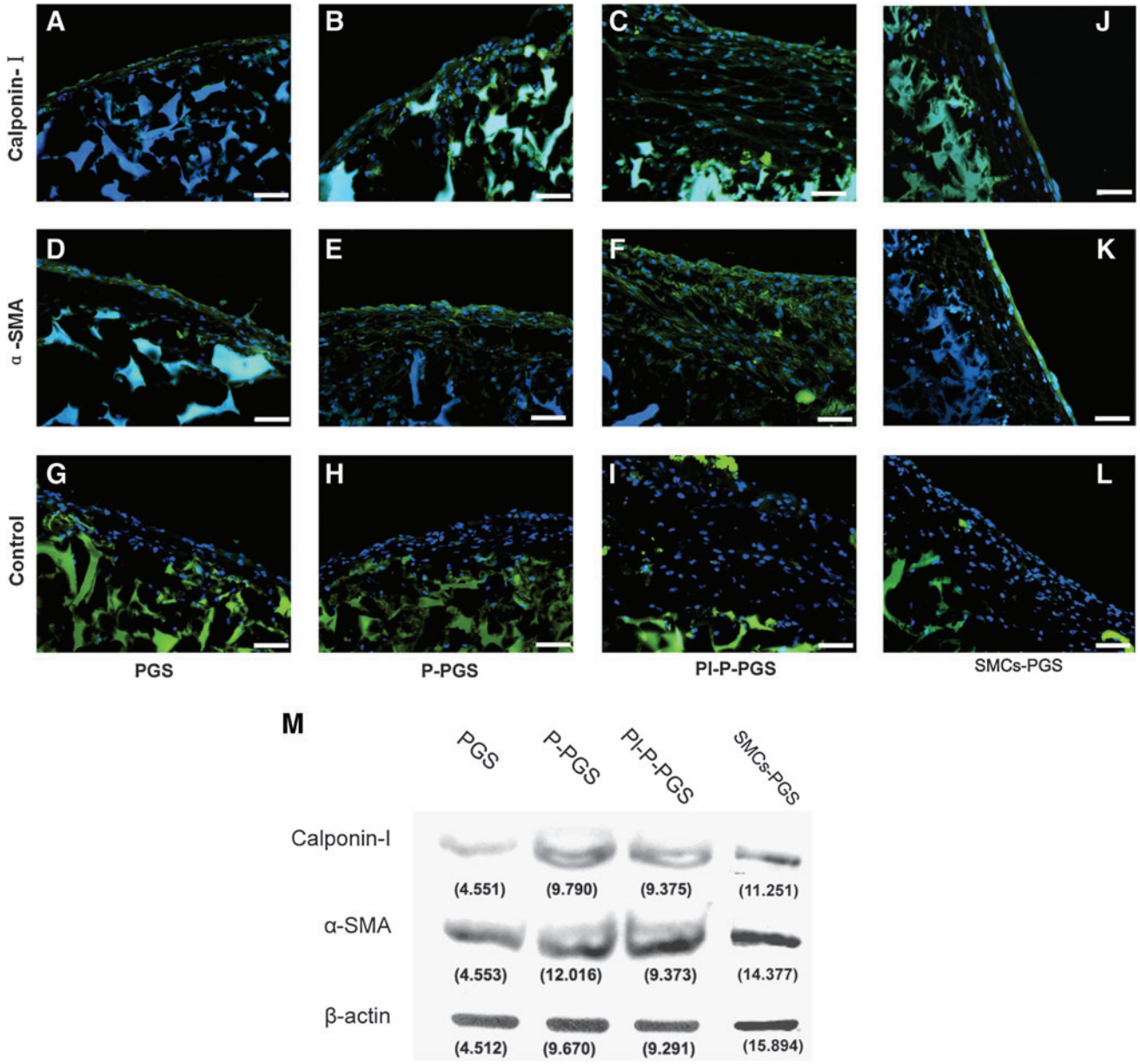

FIG. 8. **(A–F)** Immunofluorescent staining with DAPI co-stain (blue) showed expression of α-SMA and calponin-I in all constructs. **(G–I)** Constructs stained without primary antibodies (negative control) demonstrated nonspecific staining of PGS with secondary antibodies and DAPI. Pl-P-PGS constructs had the strongest expression of α-SMA and calponin-I. **(J–L)** SMCs seeded in PGS scaffolds act as positive control. 200×, scale bars = 50 μm. **(M)** Western blotting confirms α-SMA and calponin-I expression in all groups. β-actin protein levels were measured to show protein loading. α-SMA, α-smooth muscle actin; SMC, smooth muscle cell. Color images available online at www.liebertonline.com/tea

scaffolds. Masson's trichrome staining revealed the presence of collagen (blue) in the constructs (Fig. 6C, bottom panel). Cells (brownish red) showed spindle morphology and were surrounded by ECM. Increased cellularity in Pl-P-PGS was further confirmed by image analysis with Nikon Elements software to calculate cell density per unit area (Fig. 6D); Pl-P-PGS constructs contained twice as many cells per unit area as PGS constructs ($p < 0.01$). P-PGS constructs also showed ~40% higher cell density than PGS ($p < 0.01$). Further, platelet treatment significantly improved cellularity over platelet-poor plasma coating alone ($p < 0.05$). Anti–von Willebrand factor immunofluorescent staining revealed the presence of platelets at 21 days culture in Pl-P-PGS scaffolds, indicating their potential to affect tissue formation for long periods of culture (Fig. 6E).

As Figure 7 indicates, osteochondrogenic differentiation of BMNCs in PLGA scaffolds was shown by H&E, Masson's trichrome, von Kossa staining, and ALP activity. Calcium deposition is evident in Figure 7C as dark spots distributed throughout the constructs. After 14 days of incubation, cells in PLGA scaffolds showed significantly higher ALP activity than cells in PGS groups, $p < 0.01$. No cells cultured on PGS scaffolds showed osteochondrogenic differentiation.

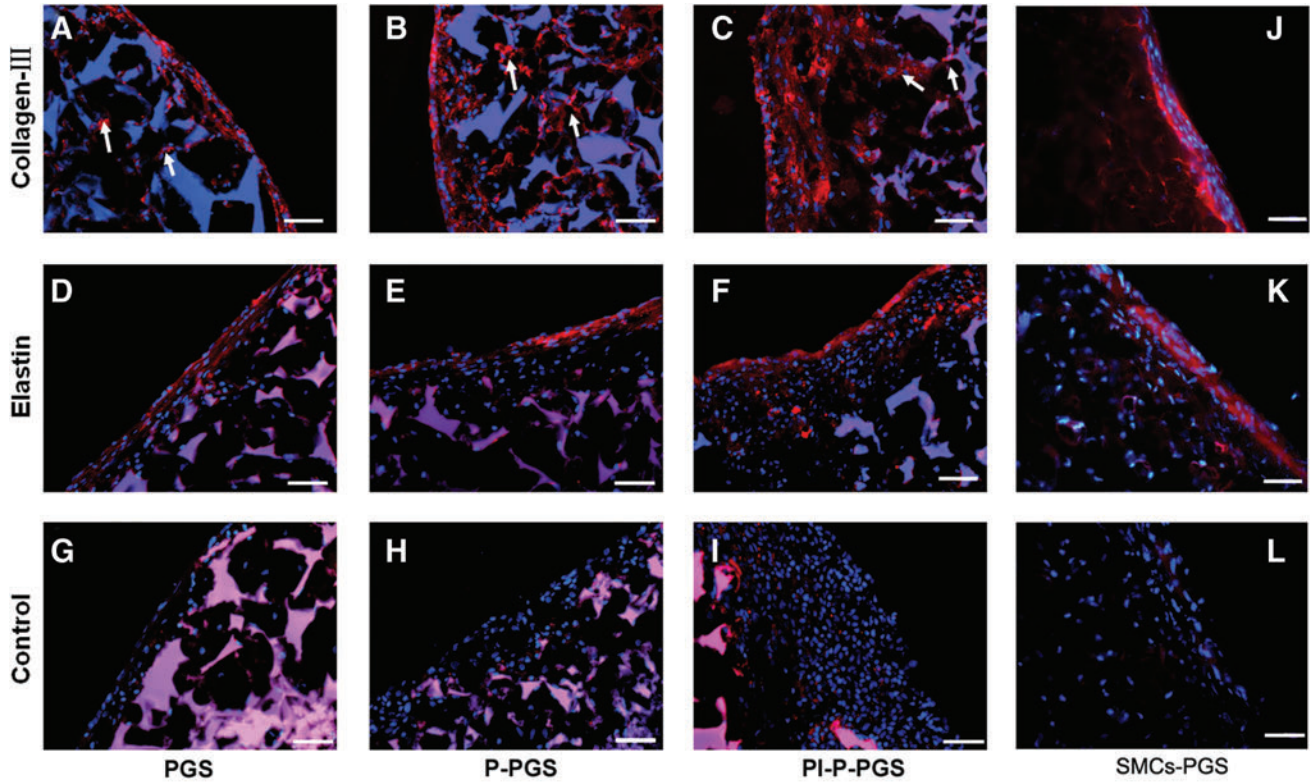
Collagen-III
Elastin
Control
A
B
C
J
D
E
F
K
G
H
I
L
PGS
P-PGS
PI-P-PGS
SMCs-PGS

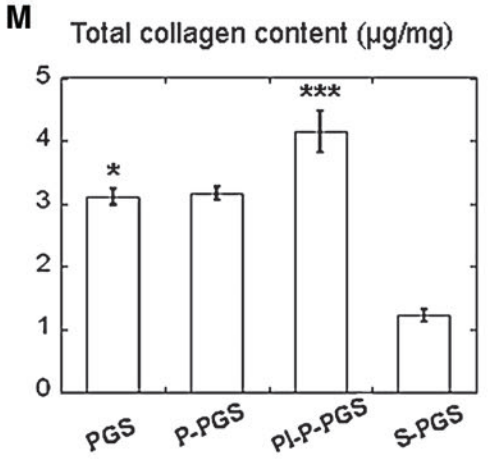
M
Total collagen content (μg/mg)
5
4
3
2
1
0
*
***
PGS
P-PGS
PI-P-PGS
S-PGS

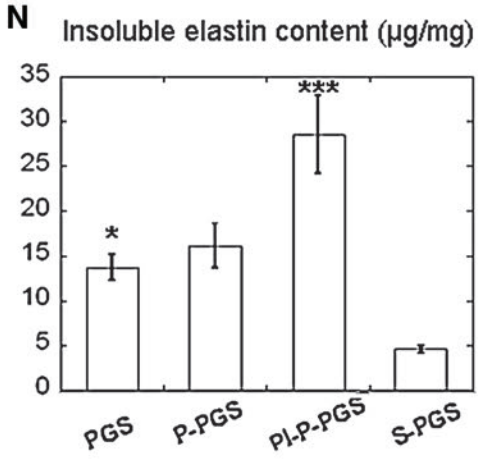
N
Insoluble elastin content (μg/mg)
35
30
25
20
15
10
5
0
*
***
PGS
P-PGS
PI-P-PGS
S-PGS

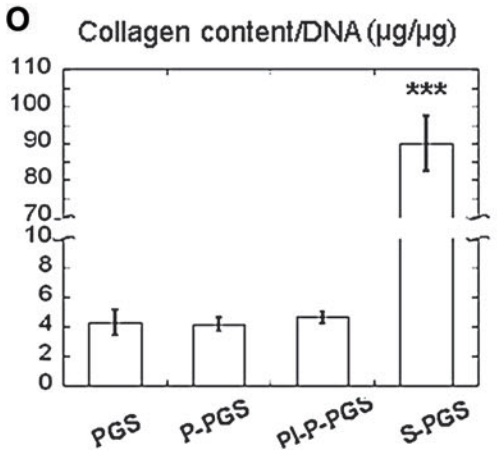
O
Collagen content/DNA (μg/μg)
110
100
90
80
70
10
8
6
4
2
0
***
PGS
P-PGS
PI-P-PGS
S-PGS

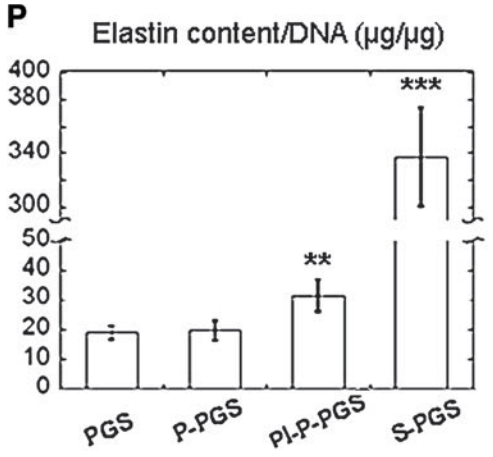
P
Elastin content/DNA (μg/μg)
400
380
340
300
50
40
30
20
10
0
**
***
PGS
P-PGS
PI-P-PGS
S-PGS

Immunofluorescent microscopy demonstrated expression of SMC markers α-SMA and calponin-I in all PGS constructs (Fig. 8A–F). Cell nuclei were counterstained with DAPI. The large positive staining (blue) was due to adsorption to PGS scaffold. As expected, cells were distributed predominantly on scaffold outer surfaces and fewer cells were beneath the scaffold surface. Many cells were α-SMA and calponin-I positive, and stained similarly to the positive controls (SMC-PGS constructs) (Fig. 8J, K). Positive staining of large areas beneath the scaffold surface was due to nonspecific adsorption of secondary antibodies by PGS, as confirmed by negative controls prepared without primary antibodies (Fig. 8G–I, L). Western blots confirmed the expression of calponin-I and α-SMA in all PGS constructs, with P-PGS and Pl-P-PGS displaying higher expression of calponin-I than PGS alone (Fig. 8M). The expression of these SMC markers was confirmed by positive controls (SMC-PGS).

Moreover, the SMC-like cells also synthesized characteristic vascular proteins collagen III and elastin in all constructs (Fig. 9, DAPI counterstain). Collagen III was strongly expressed both at the surface and the interior of the constructs (Fig. 9A–C). Elastin was also strongly expressed by cells in all the constructs (Fig. 9D–F). In contrast to collagen, most of the elastin was on the construct surface with weaker elastin expression in the interior. As observed before, PGS scaffolds showed strong nonspecific adsorption of DAPI and secondary antibodies as displayed in negative controls prepared without primary antibodies (Fig. 9G–I). Quantification of collagen and elastin per construct wet weight (Fig. 9 M, N) showed that Pl-P-PGS constructs produced significantly more collagen and elastin than PGS, P-PGS, and SMC-PGS constructs ($p < 0.05$). Without platelets, plasma treatment did not significantly increase collagen ($p = 0.947$) or elastin ($p = 0.516$) content compared with untreated PGS. However, DNA content in any of the BMNC groups is much higher than that of the SMC-PGS group, and after normalization by DNA content, the SMC-PGS group produced significantly more collagen and elastin than any of the BMNC groups ($p < 0.05$). The cell seeding density is identical in all groups; thus, BMNCs proliferate faster than SMCs. Among the BMNCs groups, only Pl-P-PGS group showed significantly higher elastin content than the other groups ($p < 0.05$), and no significant difference was found in normalized collagen expression among all BMNC-seeded groups (Fig. 9O, P).

Discussion

In vivo, differentiation is controlled mainly by the local microenvironment/niche of stem cells. Therefore, a biomimetic microenvironment that can guide cell differentiation is a very powerful tool in regenerative medicine.[25] In this study, we built an artificial niche for vascular tissue formation from BMNCs by combining the soft elastomeric PGS and platelets and plasma. We found that diluted platelet-poor plasma and platelets could be coated onto the porous structure of the PGS scaffolds. Dynamic culture on PGS scaffolds showed that (1) BMNCs grown in bare PGS scaffolds expressed characteristic SMC proteins, SMC morphology, and secreted arterial ECM without adding growth factors other than those contained in FBS; (2) pretreatment with platelet-poor plasma significantly improved adhesion to PGS scaffolds; (3) scaffolds coated with platelets significantly enhanced proliferation of differentiated cells and total ECM synthesis, including elastin synthesis, thereby accelerating ECM formation.

Mechanical properties are important design criteria for scaffolds in tissue engineering. It has been widely reported that substrate mechanical properties affect the behavior of cultured cells.[13,26] This is particularly true in vascular tissue engineering; our group previously reported that seeding vascular cells onto PGS, a biodegradable elastomer with mechanical properties similar to native arteries, improved SMC expression of elastin and produced constructs with compliance more similar to native arteries compared with constructs engineered from stiffer PLGA scaffolds.[17] BMNCs contain two known stem cells—BMSCs and hematopoietic stem cells. Substrate stiffness has also been shown to affect the differentiation of BMSCs.[13] BMSCs have been shown to differentiate into both endothelial cells and SMCs using proper soluble signals.[11,27] On the other hand, hematopoietic stem cells can also differentiate into ECs and SMCs under hypoxia and proper growth factor signaling.[28] A key finding in this study is that the adherent population of BMNCs cultured on PGS scaffolds without additional biochemical stimulation induced expression of early and mid-stage SMC differentiation markers (the only growth factors and other bioactive molecules that may affect cell differentiation are from FBS in the regular culture medium). In contrast, BMNCs cultured on stiffer PLGA scaffolds presented osteochondrogenic differentiation, suggesting that substrate stiffness may play a role in BMNC differentiation. Another recent study also showed expression of osteochondrogenic markers when BMSCs in PLGA scaffolds underwent perfusion culture, even without induction components.[29] It was shown that high-density seeding of BMSCs in Petri dish favored chondrogensis *in vitro*,[30] and bone marrow cells in TCPS with the same cell density as on PGS constructs

FIG. 9. Immunofluorescent staining of extracellular matrix proteins in the constructs with DAPI co-stain. **(A–F)** All groups were positive for collagen III and elastin staining throughout the constructs, including within pores (arrows). Pl-P-PGS constructs **(C** and **F)** appeared to express more extracellular matrix protein than the other two groups. **(G–I)** Constructs stained without primary antibodies (negative control) showed nonspecific staining of PGS with secondary antibodies and DAPI. **(J–L)** SMCs seeded in PGS scaffolds act as positive control. 200×, scale bars = 50 μm. **(M** and **N)** Quantification of collagen and insoluble elastin in constructs normalized to construct wet weight. Pl-P-PGS groups had significantly higher protein expression than the other groups. SMC-PGS abbreviated as S-PGS in the figure, $n = 4$. $^{*}p < 0.05$ (PGS vs. S-PGS), $^{**}p < 0.05$ (P-PGS vs. PGS), $^{***}p < 0.05$ (Pl-P-PGS vs. P-PGS). **(O** and **P)** Quantification of collagen and insoluble elastin in constructs normalized by DNA content. The S-PGS group had higher collagen and elastin production than any other group. No significant differences were detected in normalized collagen content among all the bone marrow mononuclear cells groups. However, elastin/DNA in Pl-P-PGS group was significantly higher than the other groups. $n = 4$, $^{**}p < 0.05$ (P-PGS vs. PGS), $^{***}p < 0.05$ (S-PGS vs. P-PGS). Color images available online at www.liebertonline.com/tea

underwent chondrogenesis upon the exposure to 10% FBS (Supplementary Fig. S2).

We directly seeded BMNCs in the scaffolds without proliferation in Petri dishes to avoid repeated enzymatic digestion, reduce culture time, eliminate the cost of additional growth factors, and circumvent potential effects of stiff substrates on cell differentiation. A potential disadvantage of direct scaffold seeding is the reduced cell proliferation. However, if cells can proliferate well within scaffolds, this disadvantage will be mitigated. Further, bone marrow can be obtained in large quantities from iliac crest and tibia clinically, and has been widely used for reconstruction of critical-sized bone defect. Frittoli *et al.* reported that bone marrow aspirated from human iliac crest contains ~10–20 million BMNCs per mL.[31] Therefore, 10 mL of bone marrow aspirate is sufficient to construct a 10 cm graft with a 5 mm internal diameter according to the cell seeding density in the present study. Obtaining 10 mL bone marrow aspirates from human is highly feasible. Interesting questions that remain to be answered are whether the BMNC cell subpopulations captured by PGS are different from those captured by tissue culture plastic or bioceramics, and whether substrate elasticity influences cell adhesion in the absence of substrate strain.

Incorporating biochemical signals into scaffolds is a strategy often used in tissue engineering to influence the behavior of seeded cells. Platelet-mediated biochemical signals affect a variety of cell types.[21] *In vivo*, platelets initiate thrombosis and mediate the wound healing cascade.[32] Platelets promote vascular repair by releasing growth factors, including stem cell-derived factor-1α and vascular endothelial growth factor to recruit circulating EPCs.[19,20] Platelets guide recruited EPC differentiation cooperatively with fibrin.[33] Platelet-rich plasma and platelet lysate promoted the proliferation and differentiation of BMNC-derived cells both *in vitro* and *in vivo*.[34–36] We coated PGS scaffolds with platelets and found that platelets improved cell proliferation. Consequently, total synthesis of collagen and elastin was enhanced in the P-Pl-PGS construct. We also found that enrichment with plasma or plasma and platelets did not increase collagen production normalized to DNA in the constructs, which was similar to less collagen production of SMCs in PGS scaffold.[17] It is well known that elastin production *in vitro* is generally low in tissue-engineered blood vessels.[37] Our previous study showed that elastin production of SMCs was enhanced significantly in PGS scaffold as compared with PLGA.[17] Consistent with this, we found that BMNCs could produce a significant amount of elastin in PGS scaffolds, which indicated that PGS could be a suitable scaffold for stem and progenitor cell-based vascular tissue engineering. Further, we found that Pl-P-PGS group had higher elastin content than P-PGS group, which indicated that platelet addition enhanced elastin production, but plasma did not contain sufficient biological cues to improve ECM production. Tranquillo and colleagues and Kim *et al.* demonstrated that transforming growth factor β1 increased elastin synthesis in three-dimensional cultures of SMCs.[37,38] Our results are consistent with prior literature report on the importance of growth factors on elastin production because platelets contain many growth factors, including transforming growth factor β1.[21] The elastin content in various BMNC-PGS groups normalized by DNA was significantly lower than the reported values for SMC culture (89 μg/μg DNA)[39] and our own results of SMC-GPS group. This could be a consequence of lower number of differentiated SMCs or an immature phenotype of SMCs. Further research will have to be conducted to tease this out. Colazzo *et al.* recently reported that adipose-derived progenitor cells could sense mechanical stimulation and produce elastin when the substrate was stretched.[40] It is possible that cell differentiation will be further enhanced by proper mechanical stimulation in our system as well.

We expected that pretreatment with Pl-P would further improve cell capture because platelets and fibrin cooperatively mediate cell adhesion *in vivo*.[33] This could be attributed to the differences between cell adhesion dynamics in our *in vitro* study compared with *in vivo* conditions. Previous studies have demonstrated that platelets promote osteochondrogenesis of BMSCs *in vitro* and *in vivo*,[41–43] but osteochondrogenesis did not occur in PGS constructs. Our results indicate that platelet-induced differentiation might be coupled with signals from substrate mechanical properties. We noticed that platelets did not significantly increase the wet weight of tissue (Fig. 6E; $p = 0.098$) in our study. The lack of difference in statistics is likely caused by the small size of the construct or the limited number of samples ($n = 3$). A larger sample size would be preferable; however, our sample size was limited by the availability of rat bone marrow. Further studies using bone marrow from large animals or humans will mitigate this limitation and allow larger sample sizes and more thorough examination of potential differences among the groups.

There is no significant difference in seeding efficiency between Pl-P-PGS and P-PGS (Fig. 4G). Protein coating is a common and simple method to affect cell adhesion and behavior. Sales *et al.* found that coating PGS with different ECM proteins altered the phenotype and ECM production of EPC.[18] Platelet-poor plasma, which contains a wide variety of bioactive molecules, including coagulation proteins,[43] is an attractive source for protein precoating because it can be harvested simply and autologously from peripheral blood. In particular, plasma fibrinogen can polymerize to fibrin on biomaterial surfaces, and fibrin mediates a variety of cellular behaviors, including adhesion, proliferation, and migration.[26,44] In this study, we found that platelet-poor plasma significantly improved cell seeding efficiency (Fig. 4) and proliferation (Figs. 5E and 6D) on PGS scaffolds. *In vivo*, fibrin mediates cell adhesion directly by providing binding sites (RGD, RGDF, Mac-1 binding domains), and indirectly by promoting adhesion related behaviors.[45] Consequently, we speculate that the deposition of plasma components improved BMNC capture. Improved proliferation in P-PGS constructs may be due in part to the degradation products of plasma fibrin. Recent work has shown that fibrin degradation products improve the proliferation of entrapped vascular SMCs.[46]

Two methods of cell quantification were used in this study: crystal violet was used to count nuclei, which is a more precise measure of cell numbers. However, it is very difficult to free all the nuclei from long-term culture samples because of the large size of nuclei. Thus, for long-term culture, DNA content was used as an indicator of cell numbers. One limitation of this study is that the effects of platelets cannot be uncoupled from the effects of plasma. We did not

isolate platelets from plasma because we found that platelets became activated during centrifugation (thereby releasing many microvesicles containing growth factors), and the additional washing and resuspension steps required to separate platelets from plasma residue are likely to remove a significant amounts of growth factors.

Conclusions

We created an artificial niche for vascular differentiation of BMNCs by combining platelet-poor plasma, platelets, and PGS. Our study demonstrates that biomaterial mechanical properties and tissue repairing signals from both plasma and platelets can cooperatively guide BMNCs into smooth-muscle-like cells with phenotypic marker expression and characteristic ECM synthesis. Future study will use tubular scaffolds and investigate the effect of pulsatile distension and shear stress on construct properties. Further, the interaction between hematopoietic stem cells and PGS will be thoroughly investigated. We believe that this artificial niche could lead to a new approach in artery engineering using this direct BMNC seeding strategy.

Acknowledgments

This research was supported by NIH Grant HL089658. We thank Hunghao Chu for stimulating discussions and assistance in data analysis.

Disclosure Statement

No competing financial interests exist.

References

1. Mirzaei, M., Truswell, A.S., Taylor, R., and Leeder, S.R. Coronary heart disease epidemics: not all the same. Heart **95,** 740, 2009.
2. Comparison of coronary bypass surgery with angioplasty in patients with multivessel disease. The Bypass Angioplasty Revascularization Investigation (BARI) Investigators. N Engl J Med **335,** 217, 1996.
3. L'Heureux, N., McAllister, T.N., and de la Fuente, L.M. Tissue-engineered blood vessel for adult arterial revascularization. N Engl J Med **357,** 1451, 2007.
4. Matsumura, G., Hibino, N., Ikada, Y., Kurosawa, H., and Shin'oka, T. Successful application of tissue engineered vascular autografts: clinical experience. Biomaterials **24,** 2303, 2003.
5. Shin'oka, T., Matsumura, G., Hibino, N., Naito, Y., Watanabe, M., Konuma, T., *et al.* Midterm clinical result of tissue-engineered vascular autografts seeded with autologous bone marrow cells. J Thorac Cardiovasc Surg **129,** 1330, 2005.
6. Sata, M., Saiura, A., Kunisato, A., Tojo, A., Okada, S., Tokuhisa, T., *et al.* Hematopoietic stem cells differentiate into vascular cells that participate in the pathogenesis of atherosclerosis. Nat Med **8,** 403, 2002.
7. Moonen, J.R., Krenning, G., Brinker, M.G., Koerts, J.A., van Luyn, M.J., and Harmsen, M.C. Endothelial progenitor cells give rise to pro-angiogenic smooth muscle-like progeny. Cardiovasc Res **86,** 506, 2010.
8. Ross, J.J., Hong, Z., Willenbring, B., Zeng, L., Isenberg, B., Lee, E.H., *et al.* Cytokine-induced differentiation of multipotent adult progenitor cells into functional smooth muscle cells. J Clin Invest **116,** 3139, 2006.
9. Hibino, N., Shin'oka, T., Matsumura, G., Ikada, Y., and Kurosawa, H. The tissue-engineered vascular graft using bone marrow without culture. J Thorac Cardiovasc Surg **129,** 1064, 2005.
10. Au, P., Tam, J., Fukumura, D., and Jain, R.K. Bone marrow-derived mesenchymal stem cells facilitate engineering of long-lasting functional vasculature. Blood **111,** 4551, 2008.
11. Riha, G.M., Lin, P.H., Lumsden, A.B., Yao, Q., and Chen, C. Review: application of stem cells for vascular tissue engineering. Tissue Eng **11,** 1535, 2005.
12. Huang, N.F., and Li, S. Mesenchymal stem cells for vascular regeneration. Regen Med **3,** 877, 2008.
13. Discher, D.E., Janmey, P., and Wang, Y.L. Tissue cells feel and respond to the stiffness of their substrate. Science **310,** 1139, 2005.
14. Wang, Y., Ameer, G.A., Sheppard, B.J., and Langer, R. A tough biodegradable elastomer. Nat Biotechnol **20,** 602, 2002.
15. Roeder, R., Wolfe, J., Lianakis, N., Hinson, T., Geddes, L.A., and Obermiller, J. Compliance, elastic modulus, and burst pressure of small-intestine submucosa (SIS), small-diameter vascular grafts. J Biomed Mater Res **47,** 65, 1999.
16. Roy, S., Silacci, P., and Stergiopulos, N. Biomechanical properties of decellularized porcine common carotid arteries. Am J Physiol Heart Circ Physiol **289,** H1567, 2005.
17. Crapo, P.M., and Wang, Y. Physiologic compliance in engineered small-diameter arterial constructs based on an elastomeric substrate. Biomaterials **31,** 1626, 2010.
18. Sales, V.L., Engelmayr, G.C., Jr., Johnson, J.A., Jr., Gao, J., Wang, Y., Sacks, M.S., *et al.* Protein precoating of elastomeric tissue-engineering scaffolds increased cellularity, enhanced extracellular matrix protein production, and differentially regulated the phenotypes of circulating endothelial progenitor cells. Circulation **116,** I55, 2007.
19. Stellos, K., and Gawaz, M. Platelet interaction with progenitor cells: potential implications for regenerative medicine. Thromb Haemost **98,** 922, 2007.
20. Stellos, K., Langer, H., Daub, K., Schoenberger, T., Gauss, A., Geisler, T., *et al.* Platelet-derived stromal cell-derived factor-1 regulates adhesion and promotes differentiation of human CD34+ cells to endothelial progenitor cells. Circulation **117,** 206, 2008.
21. Foster, T.E., Puskas, B.L., Mandelbaum, B.R., Gerhardt, M.B., and Rodeo, S.A. Platelet-rich plasma: from basic science to clinical applications. Am J Sports Med **37,** 2259, 2009.
22. Gao, J., Crapo, P.M., and Wang, Y. Macroporous elastomeric scaffolds with extensive micropores for soft tissue engineering. Tissue Eng **12,** 917, 2006.
23. Marsano, A., Maidhof, R., Wan, L.Q., Wang, Y., Gao, J., Tandon, N., and Vunjak-Novakovic, G. Scaffold stiffness affects the contractile function of three-dimensional engineered cardiac constructs. Biotechnol Prog **26,** 1382, 2010.
24. Nasseri, B.A., Pomerantseva, I., Kaazempur-Mofrad, M.R., Sutherland, F.W., Perry, T., Ochoa, E., *et al.* Dynamic rotational seeding and cell culture system for vascular tube formation. Tissue Eng **9,** 291, 2003.
25. Tenney, R.M., and Discher, D.E. Stem cells, microenvironment mechanics, and growth factor activation. Curr Opin Cell Biol **21,** 630, 2009.
26. Seib, F.P., Prewitz, M., Werner, C., and Bornhauser, M. Matrix elasticity regulates the secretory profile of human

bone marrow-derived multipotent mesenchymal stromal cells (MSCs). Biochem Biophys Res Commun **389,** 663, 2009.
27. Gong, Z., and Niklason, L.E. Small-diameter human vessel wall engineered from bone marrow-derived mesenchymal stem cells (hMSCs). FASEB J **22,** 1635, 2008.
28. Berthelemy, N., Kerdjoudj, H., Schaaf, P., Prin-Mathieu, C., Lacolley, P., Stoltz, J.F., *et al.* O2 level controls hematopoietic circulating progenitor cells differentiation into endothelial or smooth muscle cells. PLoS One **4,** e5514, 2009.
29. Yang, J., Cao, C., Wang, W., Tong, X., Shi, D., Wu, F., Zheng, Q., Guo, C., Pan, Z., Gao, C., and Wang, J. Proliferation and osteogenesis of immortalized bone marrow-derived mesenchymal stem cells in porous polylactic glycolic acid scaffolds under perfusion culture. J Biomed Mater Res A **92,** 817, 2010.
30. Koga, H., Muneta, T., Nagase, T., Nimura, A., Ju, Y.J., Mochizuki, T., *et al.* Comparison of mesenchymal tissues-derived stem cells for *in vivo* chondrogenesis: suitable conditions for cell therapy of cartilage defects in rabbit. Cell Tissue Res **333,** 207, 2008.
31. Frittoli, M.C., Biral, E., Cappelli, B., Zambelli, M., Roncarolo, M.G., Ferrari, G., Ciceri, F., *et al.* Bone marrow as a source of hematopoietic stem cells for human gene therapy of β-thalassemia. Hum Gene Ther 2011 [Epub ahead of print]; DOI:10.1089/hum.2010.045.
32. Freedman, J.E. Molecular regulation of platelet-dependent thrombosis. Circulation **112,** 2725, 2005.
33. de Boer, H.C., Verseyden, C., Ulfman, L.H., Zwaginga, J.J., Bot, I., Biessen, E.A., *et al.* Fibrin and activated platelets cooperatively guide stem cells to a vascular injury and promote differentiation towards an endothelial cell phenotype. Arterioscler Thromb Vasc Biol **26,** 1653, 2006.
34. Vogel, J.P., Szalay, K., Geiger, F., Kramer, M., Richter, W., and Kasten, P. Platelet-rich plasma improves expansion of human mesenchymal stem cells and retains differentiation capacity and *in vivo* bone formation in calcium phosphate ceramics. Platelets **17,** 462, 2006.
35. Zaky, S.H., Ottonello, A., Strada, P., Cancedda, R., and Mastrogiacomo, M. Platelet lysate favours *in vitro* expansion of human bone marrow stromal cells for bone and cartilage engineering. J Tissue Eng Regen Med **2,** 472, 2008.
36. van den Dolder, J., Mooren, R., Vloon, A.P., Stoelinga, P.J., and Jansen, J.A. Platelet-rich plasma: quantification of growth factor levels and the effect on growth and differentiation of rat bone marrow cells. Tissue Eng **12,** 3067, 2006.
37. Long, J.L., and Tranquillo, R.T. Elastic fiber production in cardiovascular tissue-equivalents. Matrix Biol **22,** 339, 2003.
38. Kim, P.D., Peyton, S.R., VanStrien, A.J., and Putnam, A.J. The influence of ascorbic acid, TGF-beta1, and cell-mediated remodeling on the bulk mechanical properties of 3-D PEG-fibrinogen constructs. Biomaterials **30,** 3854, 2009.
39. Ramamurthi, A., and Vesely, I. Evaluation of the matrix-synthesis potential of crosslinked hyaluronan gels for tissue engineering of aortic heart valves. Biomaterials **26,** 999, 2005.
40. Colazzo, F., Sarathchandra, P., Smolenski, R.T., Chester, A.H., Tseng, Y.T., Czernuszka, J.T., Yacoub, M.H., and Taylor, P.M. Extracellular matrix production by adipose-derived stem cells: implications for heart valve tissue engineering. Biomaterials **32,** 119, 2011.
41. Kasten, P., Vogel, J., Luginbuhl, R., Niemeyer, P., Weiss, S., Schneider, S., *et al.* Influence of platelet-rich plasma on osteogenic differentiation of mesenchymal stem cells and ectopic bone formation in calcium phosphate ceramics. Cells Tissues Organs **183,** 68, 2006.
42. Chevallier, N., Anagnostou, F., Zilber, S., Bodivit, G., Maurin, S., Barrault, A., *et al.* Osteoblastic differentiation of human mesenchymal stem cells with platelet lysate. Biomaterials **31,** 270, 2010.
43. Thadikkaran, L., Siegenthaler, M.A., Crettaz, D., Queloz, P.A., Schneider, P., and Tissot, J.D. Recent advances in blood-related proteomics. Proteomics **5,** 3019, 2005.
44. Tschoeke, B., Flanagan, T.C., Koch, S., Harwoko, M.S., Deichmann, T., Ellå, V., *et al.* Tissue-engineered small-caliber vascular graft based on a novel biodegradable composite fibrin-polylactide scaffold. Tissue Eng Part A **15,** 1909, 2009.
45. Mosesson, M.W. Fibrinogen and fibrin structure and functions. J Thromb Haemost **3,** 1894, 2005.
46. Ahmann, K.A., Weinbaum, J.S., Johnson, S., and Tranquillo, R.T. Fibrin degradation enhances vascular smooth muscle cell proliferation and matrix deposition in fibrin-based tissue constructs fabricated in vitro. Tissue Eng Part A **16,** 3261, 2010.

Address correspondence to:
Yadong Wang, Ph.D.
University of Pittsburgh
3700 O'Hara St.
Pittsburgh, PA 15261

E-mail: yaw20@pitt.edu

Received: September 17, 2010
Accepted: March 28, 2011
Online Publication Date: May 4, 2011